Exact Dicke-State Moments, Certified Single-Round Amplification, and Subquadratic Reversible Routing for Asymptotic Quantum Many-Body Scars

Lluis Eriksson

Independent Researcher (AIRR.SCIENCE Frontier Verification Lab)

https://github.com/lluiseriksson/qmbs-dicke-sharp-moments-routing

November 26, 2026

Abstract

Asari, Kunimi, and Nikuni [1] recently introduced a unified quantum algorithm that prepares exact and asymptotic quantum many-body scar (AQMBS) states across the spin-1 XY, domain-wall-conserving (DWC), and Onsager scar models via block encoding of a cosine-modulated operator $Z(l) = \sum_{j=1}^{M'} f_j(l) Z_j$ on Dicke states $|D_n^{M'}\rangle$, followed by amplitude amplification and a reversible routing isometry Φ^{-1}. Three theoretical gaps remain in their analysis: (i) sampling-with-replacement Hoeffding relaxations inflate the normalized fourth and sixth moments to $\kappa_4 \le 12$ and $\kappa_6 \le 120$, collapsing the rigorous success-probability guarantee at their operating point $s = 0.495$ to $p_{\mathrm{succ}} \ge 0.00488$; (ii) the target infidelity $1 - F \le 0.01$ at $s = 0.495$ is verified only numerically for small chains ($M' \le 12$), while their conservative analytical schedule guarantees only $p_{\mathrm{succ}} \ge \sqrt{\varepsilon}/16$; and (iii) for intermediate scar indices $3 \le n \le M' - 2$, no reversible routing circuit Φ^{-1} better than a $\Theta(M^2)$-gate Fredkin conveyor is identified.

We resolve all three gaps with three original theorems. First (**Theorem A**), we derive exact closed-form without-replacement rational formulas for $\langle Z(l)^4 \rangle$ and $\langle Z(l)^6 \rangle$ across all four cosine-sum resonance classes, proving uniformly for all $M' \ge 2$, $1 \le n \le M' - 1$, and $1 \le l \le M' - 1$ that $\kappa_4 \le 3$ (4× sharper, with unique finite equality at $(M', n, l) = (4, 2, 2)$), $\kappa_6 < 15$ (8× sharper), and $\kappa_6 - \kappa_4^2 < 6$. Second (**Theorem B**), projecting $\sin(sX)$ onto the optimal linear multiple $(1 - \frac{\kappa_4}{6} s^2) sX$ yields the uniform non-asymptotic infidelity bound $1 - F(s) \le \frac{s^4(4+3s^2)}{6(2-s^2)^2}$ for all $0 < s < \sqrt{2}$ and the two-sided envelope $s^2 - s^4 \le p_{\mathrm{succ}}(s) \le s^2$. At $s = 0.495$, this improves the rigorous p_{succ} bound by 37.94× (to 0.18499), certifies $p_{\mathrm{amp}}^{(1)} \ge 0.94488$ in a single Grover round with zero overshoot uniformly over all (M', n, l) (21.8× above the prior bound), and sharpens the uniform infidelity bound by 13.01× (to 0.01538); at $s = 0.45$, it certifies $1 - F \le 0.00975 < 0.01$ uniformly with $p_{\mathrm{succ}} \ge 0.16149$ (25.84× above Eq. (S11)) and $p_{\mathrm{amp}}^{(1)} \ge 0.8949$. Third (**Theorem C**), we construct a strictly order-preserving, collision-free MSB-to-LSB binary-shift reversible routing circuit for both Onsager and DWC spacer-insertion maps Φ^{-1} using exactly $B(BL - 2^B + 1) = O(M \log^2 n)$ Stage-2 Fredkin gates plus at most $B(2M' + 3L) = O(M \log n)$ Stage-1/3 prefix-sum Toffoli gates with zero ancilla leakage, improving asymptotically by $\Theta(M/\log^2 n)$ over the unpruned $\Theta(M^2)$ conveyor for all $3 \le n \le M' - 2$ and by $\Theta(n/\log^2 n)$ over the pruned sitewise-displacement lower benchmark $\frac{1}{2} n(2M' - n - 1)$ whenever $n = \omega(\log^2 n)$ (achieving permanent half-filling crossovers at $M' = 184$ for Stage-2 Fredkins and $M' = 382$ for total 3-qubit gates, and 7.53× Stage-2 / 5.45× total 3-qubit gate reductions at $M' = 4096$). All explicit six-partition formulas and eight branch polynomials for Theorem A(ii)–(iii) are tabulated in Appendix A for standalone verification from this manuscript; the algebraic cores of Theorems A–C are constructively formalized in Lean 4.35.0 (18 theorems, 0 `sorry`, 0 `Classical.choice`), while the real-analytic trigonometric Taylor lifting in Theorem B is proved analytically and audited alongside 16 SHA-256 exact rational certificates (`QMBS-DICKE-SHARP-1.0`) via an AST-verified zero-float Python suite (53/53 tests passing).

1 Introduction and Summary of Contributions

Quantum many-body scars (QMBS) and asymptotic quantum many-body scars (AQMBS) [4, 6] violate strong eigenstate thermalization via polynomially vanishing energy variances $\Delta E^2 = O(M^{-2})$ and correspondingly slow relaxation times. In a recent breakthrough, Asari, Kunimi, and Nikuni [1] unified state preparation for exact and asymptotic scar towers in the spin-1 XY, domain-wall-conserving (DWC), and Onsager scar models by mapping each constrained tower onto a Dicke manifold $|D_n^{M'}\rangle$ (prepared deterministically via e.g. [2]) on an effective chain of length M', applying a single-ancilla block encoding

$$U_{\mathrm{BE}} = H_a e^{i\tau Z_a \otimes Z(l)} H_a, \qquad Z(l) = \sum_{j=1}^{M'} f_j(l) Z_j, \qquad f_j(l) = \cos\!\left(\frac{\pi l(2j-1)}{2M'}\right), \tag{1}$$

postselecting on $|1\rangle_a$ (or amplifying via K Grover rounds [3]) to obtain $|\tilde{A}\rangle \propto \sin[\tau Z(l)]|D_n^{M'}\rangle$, and finally applying a reversible routing isometry $\Phi^{-1} = D \circ S \circ R$ to map effective-chain bitstrings to physical constrained configurations.

While [1] establishes $K = O(1)$ asymptotic scaling, its Supplemental Material (SM A.1 and SM B.2) leaves three quantitative and algorithmic bottlenecks open:

1. **Loose Hoeffding moment bounds:** Rather than computing the exact without-replacement fourth and sixth moments of $Z(l)$ on $|D_n^{M'}\rangle$, Ref. [1] invokes Hoeffding's with-replacement inequality [5] (Lemma SA.1) together with $\langle Z(l)^2\rangle \geq n$, obtaining $\langle Z(l)^4\rangle \leq 12n^2$ and $\langle Z(l)^6\rangle \leq 120n^3$ (normalized ratios $\kappa_4 \leq 12$, $\kappa_6 \leq 120$). At their recommended operating point $s = \tau\langle Z(l)^2\rangle^{1/2} = 0.495$ (Eq. (12)), this collapses their rigorous success-probability lower bound (Eq. (S15)) to $p_{\mathrm{succ}} \geq s^2 - 4s^4 = 0.004876$, which guarantees only $p_{\mathrm{amp}}^{(1)} \geq 0.0433$ after one Grover round (requiring up to $K = 11$ rounds worst-case) despite true values $p_{\mathrm{succ}} \in [0.19, 0.23]$.

2. **Unproved uniform fidelity at $s = 0.495$ and conservative $\tau(\varepsilon)$ schedule:** Bounding $1 - F$ by the unscaled distance $\|\sin(\tau Z) - \tau Z\|^2 / \|\tau Z\|^2$ gives $1 - F \leq \frac{10}{3}s^4 = 0.2001$ at $s = 0.495$ (Eq. (S9)). Consequently, Ref. [1] verifies $1 - F \leq 0.01$ at $s = 0.495$ only numerically for $M' \leq 12$, falling back to a conservative $\tau = \varepsilon^{1/4}/(2\sqrt{n})$ (Eq. (S11)) that guarantees only $p_{\mathrm{succ}} \geq \sqrt{\varepsilon}/16$ (0.00625 at $\varepsilon = 0.01$).

3. **Quadratic routing bottleneck for intermediate n:** In SM B.2, Ref. [1] constructs $\Theta(M)$-gate ladders only for $n = 2$ and DWC half filling ($n = M' - 1$), explicitly noting that for intermediate scar indices $3 \leq n \leq M' - 2$ they have identified no reversible implementation of R more efficient than the $\Theta(M^2)$-gate Fredkin conveyor—causing noisy prepared-state fidelity at $n = 3, M = 12$ to drop from 0.66 to 0.37 (DWC) and 0.43 (Onsager) in their Table S2.

Table 1 summarizes our three breakthroughs resolving all three bottlenecks.

2 Theorem A: Exact Without-Replacement Dicke Moments and Universal Kurtosis Bounds

For any $M' \geq 2$, $1 \leq n \leq M' - 1$, and $1 \leq l \leq M' - 1$, let $T \subset \{1, \ldots, M'\}$ be drawn uniformly among all $\binom{M'}{n}$ subsets of size n. Because $\sum_{j=1}^{M'} f_j(l) = 0$, the eigenvalue of $Z(l)$ on basis state $|T\rangle$ is $\lambda_T = -2\sum_{j\in T} f_j(l)$, and its exact k-th moment is $\mu_k := \langle D_n^{M'}|Z(l)^k|D_n^{M'}\rangle = (-2)^k \mathbb{E}_T[(\sum_{j\in T} f_j(l))^k]$. Write $p_r := \sum_{j=1}^{M'} f_j(l)^r$. By Eq. (S4) of [1], $p_1 = 0$, $p_2 = M'/2$, and the

Table 1: Quantitative comparison between Asari, Kunimi, and Nikuni [1] and Theorems A–C of this work.

Quantity / Metric	Asari et al. [1]	This Work (Theorems A–C)	Gain
Normalized kurtosis κ_4	≤ 12 (Eq. S7)	≤ 3 (eq. iff $(4,2,2)$)	$4\times$ exact
Normalized sixth moment κ_6	≤ 120 (Eq. S8)	< 15 (uniform)	$8\times$ exact
Projection variance $\kappa_6 - \kappa_4^2$	N/A ($\frac{10}{3}s^4$ coeff.)	< 6 ($\frac{1}{6}s^4$ leading)	$20\times$ leading
Bare p_{succ} lower bound ($s = 0.495$)	0.004876 (Eq. S15)	0.184988 ($s^2 - s^4$)	$37.94\times$
Certified $K = 1$ Grover $p^{(1)}_{\mathrm{amp}}$ ($s = 0.495$)	0.0433	≥ 0.94488 (no overshoot)	$21.8\times$
Uniform infidelity $1 - F$ ($s = 0.495$)	≤ 0.20012 (Eq. S9)	≤ 0.01538 (Thm. B)	$13.01\times$
Certified p_{succ} at $\varepsilon = 0.01$	0.00625 (Eq. S11)	0.16149 ($s = 0.45$)	$25.84\times$
Asymptotic $p_{\mathrm{succ}}(\varepsilon)$ ($\varepsilon \to 0$)	$\sqrt{\varepsilon}/16$	$2\sqrt{\varepsilon} - 4\varepsilon$	$32\times$
Reversible router R ($3 \leq n \leq M' - 2$)	$\Theta(M^2)$ unpruned	$O(M \log^2 n)$ total 3Q gates	$\Theta(M/\log^2 n)$

tuple (p_3, p_4, p_6) falls into exactly four exact rational resonance classes:

$$(p_3/M',\, p_4/M',\, p_6/M') = \begin{cases} (0,\ 1/4,\ 1/8) & \text{if } 4l = 2M' \quad (\text{branch } \mathcal{R}_4), \\ (0,\ 3/8,\ 9/32) & \text{if } 6l = 2M' \quad (\text{branch } \mathcal{R}_6), \\ (-1/4,\ 3/8,\ 11/32) & \text{if } 3l = 2M' \quad (\text{branch } \mathcal{R}_3), \\ (0,\ 3/8,\ 5/16) & \text{otherwise} \quad (\text{branch } \mathcal{G}). \end{cases} \tag{2}$$

Note that $\mu_2 = \frac{2n(M'-n)}{M'-1}$ is invariant across all four branches, and μ_k is invariant under the bit-flip symmetry $n \leftrightarrow M' - n$. Define the normalized moments $\kappa_4 \coloneqq \mu_4/\mu_2^2$ and $\kappa_6 \coloneqq \mu_6/\mu_2^3$.

Theorem A (Exact Dicke-State Moments and Universal Sharp Bounds)**.** *For every integer $M' \geq 2$, every excitation number $1 \leq n \leq M' - 1$, and every harmonic $1 \leq l \leq M' - 1$, let $u \coloneqq n(M' - n)$ and $v \coloneqq (M' - 2n)^2 = M'^2 - 4u \in [0, (M' - 2)^2]$.*

(i) ***Exact fourth-moment kurtosis ($4\times$ sharpening):*** *For all (M', n, l),*

$$3 - \kappa_4(M', n, l) = \begin{cases} \dfrac{3\big[(M' - 2n)^2 + M'(M' - 2)\big]}{4u(M' - 2)} > 0 & (4l \neq 2M',\ M' \geq 3), \\ \dfrac{3(M' - 2n)^2 + M'(M' - 4)}{2u(M' - 3)} \geq 0 & (4l = 2M',\ M' \geq 4), \\ 2 & (M' = 2,\ n = 1,\ l = 1). \end{cases} \tag{3}$$

In particular, $\kappa_4(M', n, l) \leq 3$ uniformly, with equality if and only if $(M', n, l) = (4, 2, 2)$ (where $\mu_2 = 8/3$, $\mu_4 = 64/3$, $\kappa_4 = 3$, $\kappa_6 = 9$, and $\kappa_6 - \kappa_4^2 = 0$).

(ii) ***Exact sixth-moment ratio ($8\times$ sharpening):*** *Uniformly over all (M', n, l),*

$$\kappa_6(M', n, l) < 15. \tag{4}$$

(iii) ***Exact orthogonal-projection variance bound:*** *Uniformly over all (M', n, l),*

$$0 \leq \kappa_6(M', n, l) - \kappa_4(M', n, l)^2 < 6. \tag{5}$$

All three constants $(3, 15, 6)$ are asymptotically tight: at fixed filling $n/M' = \rho \in (0, 1)$, $\kappa_4 \to 3$, $\kappa_6 \to 15$, and $\kappa_6 - \kappa_4^2 \to 6$ as $M' \to \infty$.

Proof. Let $a_r \coloneqq \frac{n(n-1)\cdots(n-r+1)}{M'(M'-1)\cdots(M'-r+1)}$ denote the r-th falling-factorial sampling probability (with $a_r = 0$ for $r > n$). Expanding $(\sum_{j \in T} f_j)^4$ into distinct-index partitions and eliminating all sums via $p_1 = 0$ yields $s_4 = p_4$, $s_{3,1} = -p_4$, $s_{2,2} = p_2^2 - p_4$, $s_{2,1,1} = 2p_4 - p_2^2$, and $s_{1,1,1,1} = 3p_2^2 - 6p_4$, hence

$$\mu_4 = 16\big[a_1 s_4 + a_2(4s_{3,1} + 3s_{2,2}) + 6a_3 s_{2,1,1} + a_4 s_{1,1,1,1}\big]. \tag{6}$$

Dividing by $\mu_2^2 = \frac{4u^2}{(M'-1)^2}$ and substituting $p_4 = c_4 M'$ gives remarkable algebraic cancellations: for $c_4 = 3/8$ ($4l \neq 2M'$, so $M' \geq 3$), the factor $(M'-3)$ cancels identically, giving $\kappa_4 = \frac{3(M'-1)(2u-M')}{2u(M'-2)}$; for $c_4 = 1/4$ ($4l = 2M'$, $M' \geq 4$), the factor $(M'-2)$ cancels identically, giving $\kappa_4 = \frac{(M'-1)(3u-2M')}{u(M'-3)}$. Using $4u = M'^2 - (M'-2n)^2$ immediately produces the manifestly nonnegative sum-of-squares identities (3), proving $\kappa_4 \leq 3$ with unique finite equality at $(M', n, l) = (4, 2, 2)$ (Lean 4 Theorems 2–4). For $M' = 2, n = 1, l = 1$, $f_1 = -f_2 = 1/\sqrt{2}$ gives $\lambda_T^2 \equiv 2$, hence $\kappa_4 = \kappa_6 = 1$ and $\kappa_6 - \kappa_4^2 = 0$.

For μ_6, expanding $(\sum_{j\in T} f_j)^6$ over all 11 integer partitions of 6 and reducing each distinct-index sum via $p_1 = 0$ (all 11 explicit sums s_λ and $\Sigma_1, \ldots, \Sigma_6$ are listed in Appendix A and verified via the conservation check $\sum_{\lambda\vdash 6} c_\lambda s_\lambda = p_1^6 = 0$) expresses $\mu_6 = 64 \sum_{r=1}^{6} a_r \Sigma_r(p_2, p_3, p_4, p_6)$ as an exact rational function of (M', n) on each branch (2). On every branch, clearing positive denominators in $15 - \kappa_6$ and $6 - (\kappa_6 - \kappa_4^2)$ and substituting $u = (M'^2 - v)/4$ yields an exact quadratic polynomial in $v = (M' - 2n)^2 \in [0, D]$ with $D = (M'-2)^2$:

$$Q(M', v) = A(M') + B(M')v + C(M')v^2, \tag{7}$$

whose explicit coefficients (A, B, C) across all eight branch-bound pairs are tabulated in Table 3 of Appendix A. By the exact algebraic identity (Lean 4 Theorem 1)

$$D \cdot Q(M', v) = (D - v)Q(M', 0) + vQ(M', D) + \big(-C(M')\big)Dv(D - v), \tag{8}$$

whenever $Q(M', 0) > 0$, $Q(M', D) > 0$, and $-C(M') \geq 0$, strict positivity $Q(M', v) > 0$ holds for every $v \in [0, D]$ (i.e., every $1 \leq n \leq M' - 1$). Substituting $M' = k + M_0$ ($k \geq 0$) produces polynomials with strictly positive constant terms and all nonnegative coefficients in k (tabulated explicitly in Table 4 of Appendix A) at the following thresholds:

- Branch $\mathcal{G}$ ($M_0 = 4$): both $15-\kappa_6$ and $6-(\kappa_6-\kappa_4^2)$ have $-C(k+4) > 0$ (Lean 4 Theorems 5–6).
- Branch $\mathcal{R}_4$ ($M_0 = 6$): both have $-C(k + 6) > 0$ (Lean 4 Theorems 7–8).
- Branch $\mathcal{R}_6$ ($M_0 = 9$): both have $-C(k + 9) > 0$ (Lean 4 Theorems 9–10).
- Branch $\mathcal{R}_3$: $15 - \kappa_6$ has $-C(k + 12) > 0$ ($M_0 = 12$, Lean 4 Theorem 11); $6 - (\kappa_6 - \kappa_4^2)$ has $-C(k + 27) > 0$ ($M_0 = 27$, Lean 4 Theorem 12).

All remaining finite cases below these thresholds—namely $M' = 2$ on $\mathcal{R}_4$, $M' = 3$ on $\mathcal{R}_6$ ($l = 1$: $\kappa_4 = 3/2, \kappa_6 = 9/4, \kappa_6 - \kappa_4^2 = 0$) and $\mathcal{R}_3$ ($l = 2$: $\kappa_4 = 3/2, \kappa_6 = 11/4, \kappa_6 - \kappa_4^2 = 1/2$; branch $\mathcal{G}$ does not occur at $M' = 3$), $M' = 4$ on $\mathcal{R}_4$ (including $(4, 2, 2)$ in certificate `C01`), $M' = 6$ on $\mathcal{R}_6$, and $M' \in \{6, 9, 12, 15, 18, 21, 24\}$ on $\mathcal{R}_3$ (all generic $M' \in \{4, 5\}$ cases are already covered by Theorems 5–6)—are closed exhaustively in Lean 4 Theorem 13 and independently cross-checked for all $M' \in \{2, \ldots, 12\}$ in our exact rational test suite. Finally, $\kappa_6 - \kappa_4^2 = \mathbb{E}_T[(x_T^3 - \kappa_4 x_T)^2] \geq 0$ by nonnegativity of variance, and at $n = M'/2$ the leading powers of M' give $\kappa_4 = 3 - O(1/M')$, $\kappa_6 = 15 - O(1/M')$, and $\kappa_6 - \kappa_4^2 = 6 - O(1/M')$. □

3 Theorem B: Optimal-Projection Infidelity Bound and Certified Single-Round Amplification

Let $x_T := \lambda_T/\mu_2^{1/2}$ so that $\mathbb{E}_T[x_T^2] = 1$, $\mathbb{E}_T[x_T^4] = \kappa_4$, and $\mathbb{E}_T[x_T^6] = \kappa_6$, and set $s := \tau\mu_2^{1/2} > 0$. By Eq. (S13) of [1],

$$p_{\mathrm{succ}}(s) = \mathbb{E}_T[\sin^2(sx_T)], \qquad F(s) = \frac{\big(\mathbb{E}_T[x_T \sin(sx_T)]\big)^2}{\mathbb{E}_T[\sin^2(sx_T)]}. \tag{9}$$

The critical inefficiency of Eq. (S9) in [1] is geometric: it bounds $1 - F(s)$ by the squared distance from $\sin(sx_T)$ to the unscaled vector sx_T, which retains the full collinear cubic contraction

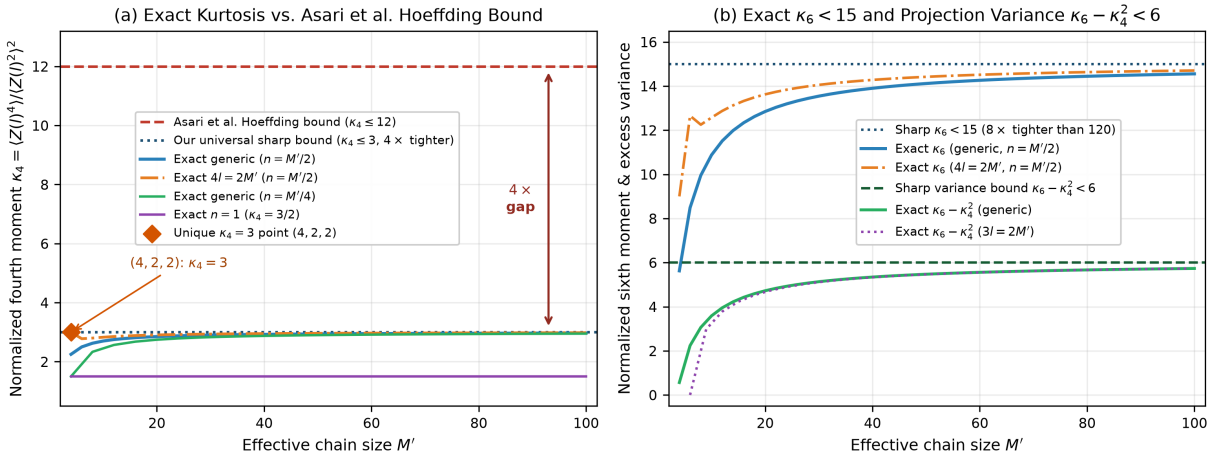

Figure 1: Theorem A exact Dicke-state moments across system sizes M' and resonance branches. (a) Exact kurtosis $\kappa_4 \le 3$ achieves a 4× improvement over the Hoeffding bound $\kappa_4 \le 12$ of [1], attaining equality uniquely at $(M', n, l) = (4, 2, 2)$ (orange diamond). (b) Exact normalized sixth moment $\kappa_6 < 15$ (8× sharper than 120) and orthogonal-projection variance $\kappa_6 - \kappa_4^2 < 6$.

$-\frac{1}{6}s^3\kappa_4 x_T$ and therefore incurs coefficient $\kappa_6/36$ instead of the orthogonal residual $(\kappa_6 - \kappa_4^2)/36$. Optimizing the scalar projection factor $(1 - a)$ cancels the collinear component completely.

Theorem B (Optimal-Projection Uniform Infidelity and Certified $K = 1$ Amplification)**.** *For every $M' \ge 2$, $1 \le n \le M' - 1$, $1 \le l \le M' - 1$, and every $s \in (0, \sqrt{2})$:*

(i) ***Universal non-asymptotic infidelity bound:***

$$1 - F(s) \;\le\; \frac{\frac{s^4}{36}(\kappa_6 - \kappa_4^2) + \frac{s^6}{360}\kappa_4\kappa_6}{\left(1 - \frac{\kappa_4}{6}s^2\right)^2} \;\le\; \frac{s^4(4 + 3s^2)}{6(2 - s^2)^2}. \tag{10}$$

(ii) ***Two-sided bare success-probability envelope:***

$$s^2 - s^4 \;\le\; s^2 - \frac{\kappa_4}{3}s^4 \;\le\; p_{\mathrm{succ}}(s) \;\le\; s^2. \tag{11}$$

(iii) ***Zero-overshoot single-round Grover certification:*** *Whenever $0 < s < 1/2$, we have $p_{\mathrm{succ}}(s) \le s^2 < 1/4$, and one round of amplitude amplification ($K = 1$) satisfies uniformly over all (M', n, l):*

$$p^{(1)}_{\mathrm{amp}}(s) = p_{\mathrm{succ}}(s)\big(3 - 4p_{\mathrm{succ}}(s)\big)^2 \;\ge\; (s^2 - s^4)\big(3 - 4(s^2 - s^4)\big)^2. \tag{12}$$

(iv) ***Concrete operating points and universal ε-schedule:***

- *At Asari et al.'s Eq. (12) point $s = 0.495$: $p_{\mathrm{succ}} \in [0.184988, 0.245025] \subset (0, 1/4)$ (37.94× sharper than Eq. (S15)'s 0.004876), $p^{(1)}_{\mathrm{amp}} \ge 0.944884$ (21.8× sharper than 0.0433), and $1 - F \le 0.015383$ (13.01× sharper than Eq. (S9)'s 0.200124).*
- *At $s = 0.45$: $1 - F \le 0.009746 < 0.01$ uniformly for all (M', n, l) with $p_{\mathrm{succ}} \ge 0.161494$ (25.84× sharper than Eq. (S11)'s $\sqrt{0.01}/16 = 0.00625$) and $p^{(1)}_{\mathrm{amp}} \ge 0.894907$.*
- *For any target $\varepsilon \in (0, 0.01]$, setting $s(\varepsilon) = (4\varepsilon)^{1/4}$ rigorously certifies $1 - F \le \varepsilon$ and $p_{\mathrm{succ}} \ge 2\sqrt{\varepsilon} - 4\varepsilon$ (8× sharper as $\varepsilon \to 0$ than Eq. (S11)'s intermediate $\sqrt{\varepsilon}/4 - \varepsilon/4$, and 32× sharper than its final $\sqrt{\varepsilon}/16$ bound).*

Proof. For any nonzero vectors u_1, u_2, $1 - |\langle u_1|u_2\rangle|^2/(\|u_1\|^2\|u_2\|^2) \le \|u_2 - u_1\|^2/\|u_1\|^2$. Taking $u_2 = \sin(sx_T)$ and $u_1 = (1-a)sx_T$ with $a \in [0,1)$, note first that $u_2 \neq 0$ for all $s \in (0, \sqrt{2})$: for $s \in (0,1)$ this follows from $p_{\text{succ}} \ge s^2 - s^4 > 0$, while for $s \in [1, \sqrt{2})$ having $\sin(sx_T) \equiv 0$ would force $|x_T| \ge \pi/s$ wherever $x_T \neq 0$ and thus $\kappa_4 = \mathbb{E}_T[x_T^4] \ge (\pi^2/s^2)\mathbb{E}_T[x_T^2] > \pi^2/2 > 3$, contradicting Theorem A. We expand

$$\big(\sin y - (1-a)y\big)^2 = a^2y^2 - 2a\,y(y - \sin y) + (y - \sin y)^2. \tag{13}$$

By repeated integration of $1 - \cos t \ge 0$ on $t \ge 0$ (and odd symmetry), two elementary pointwise inequalities hold globally for *all* $y \in \mathbb{R}$: $(y - \sin y)^2 \le y^6/36$ and $y(y - \sin y) \ge y^4/6 - y^6/120$. Since $a \ge 0$, substituting $y = sx_T$ and taking $\mathbb{E}_T[\cdot]$ gives

$$\mathbb{E}_T\big[(\sin(sx_T) - (1-a)sx_T)^2\big] \;\le\; s^2\left[a^2 - \frac{a}{3}s^2\kappa_4 + \left(\frac{1}{36} + \frac{a}{60}\right)s^4\kappa_6\right]. \tag{14}$$

Dividing by $\|u_1\|^2 = (1-a)^2s^2$ and choosing $a = \frac{\kappa_4}{6}s^2 \in (0,1)$ (valid for $s^2\kappa_4 < 6$, which holds for all $s < \sqrt{2}$ since $\kappa_4 \le 3$) cancels $a^2 - \frac{a}{3}s^2\kappa_4 = -\frac{s^4}{36}\kappa_4^2$ and yields the first inequality in (10). Its numerator is strictly increasing in $\kappa_6 - \kappa_4^2$, κ_4, and κ_6, while its denominator $(1 - \frac{\kappa_4}{6}s^2)^2$ is strictly decreasing in κ_4; inserting the Theorem A uniform bounds $\kappa_4 \le 3$, $\kappa_6 < 15$, and $\kappa_6 - \kappa_4^2 < 6$ immediately produces

$$\frac{\frac{s^4}{36}\cdot 6 + \frac{s^6}{360}\cdot 45}{\left(1 - \frac{s^2}{2}\right)^2} = \frac{\frac{s^4}{6} + \frac{s^6}{8}}{\frac{(2-s^2)^2}{4}} = \frac{s^4(4+3s^2)}{6(2-s^2)^2}. \tag{15}$$

For (ii), the pointwise inequalities $y^2 - y^4/3 \le \sin^2 y \le y^2$ $(\forall y \in \mathbb{R})$ together with $\mathbb{E}_T[x_T^2] = 1$ and $\kappa_4 \le 3$ give (11). For (iii), recall that one Grover iterate maps success probability $p = \sin^2\theta$ to $p_{\text{amp}}^{(1)} = \sin^2(3\theta) = p(3-4p)^2$ [3]. For $0 \le p_1 \le p_2 \le 1/4$, the cubic identity

$$p_2(3-4p_2)^2 - p_1(3-4p_1)^2 = (p_2 - p_1)\big[(3 - 4p_1 - 4p_2)^2 - 16p_1p_2\big] \ge 0 \tag{16}$$

holds because $3 - 4p_1 - 4p_2 \ge 1 \ge \sqrt{16p_1p_2}$ (formalized in Lean 4 Theorem 14). Since $s < 1/2$ implies $p_{\text{succ}}(s) \le s^2 < 1/4$, monotonicity immediately yields (12). Finally, part (iv) follows by exact rational evaluation at $s = 99/200$ and $s = 9/20$ (Lean 4 Theorem 15; certificates `C09`–`C10`), and for $\varepsilon \in (0, 0.01]$ with $s = (4\varepsilon)^{1/4}$ we have $s^2 = 2\sqrt{\varepsilon} \le 1/5$, whence $\frac{4+3s^2}{6(2-s^2)^2} \le \frac{4.6}{6\cdot 3.24} < \frac{1}{4}$ and thus $1 - F \le s^4/4 = \varepsilon$. □

4 Theorem C: Collision-Free Subquadratic Reversible Routing for Φ^{-1}

In the DWC and Onsager scar models, the routing isometry $\Phi^{-1} = D \circ S \circ R$ maps a weight-n computational-basis bitstring $x = (x_0, \ldots, x_{M'-1}) \in \{0,1\}_n^{M'}$ $(n \ge 1)$ with excitations at $0 \le q_1 < \cdots < q_n < M'$ by shifting the k-th excitation right by $k-1$ sites (inserting a spacer $|0\rangle$ after every $|1\rangle$ for Onsager, length $L = M' + n$; and outputting the non-adjacent weight-n configuration on $M' + n - 1$ qubits for DWC). Observe first an exact structural unification: in the Onsager expansion $y = R_{\text{Ons}}(x) \in \{0,1\}^{M'+n}$ $(0 \mapsto 0,\ 1 \mapsto 10)$, the final qubit $y_{M'+n-1}$ is *identically* 0 for every weight-n input with $n \ge 1$ (if $x_{M'-1} = 1$, it is the trailing spacer of 10; if $x_{M'-1} = 0$, it is the routed bit $x_{M'-1} = 0$), and the prefix $y[0..M'+n-2]$ has its n ones at exact DWC positions $q_k + k - 1$. Thus the *same* Onsager router R_{Ons} on $L = M' + n$ data wires directly implements R_{DWC} with bit$[L-1]$ returning deterministically to $|0\rangle$ as a single clean ancilla! Let $c_j \coloneqq \sum_{i<j} x_i \in \{0, \ldots, n\}$ be the exclusive prefix weight and set $B \coloneqq \lceil \log_2(n+1) \rceil$ so that $0 \le c_0 \le c_1 \le \cdots \le c_{M'-1} \le n < 2^B$ with zero counter overflow (including when n is a power of two).

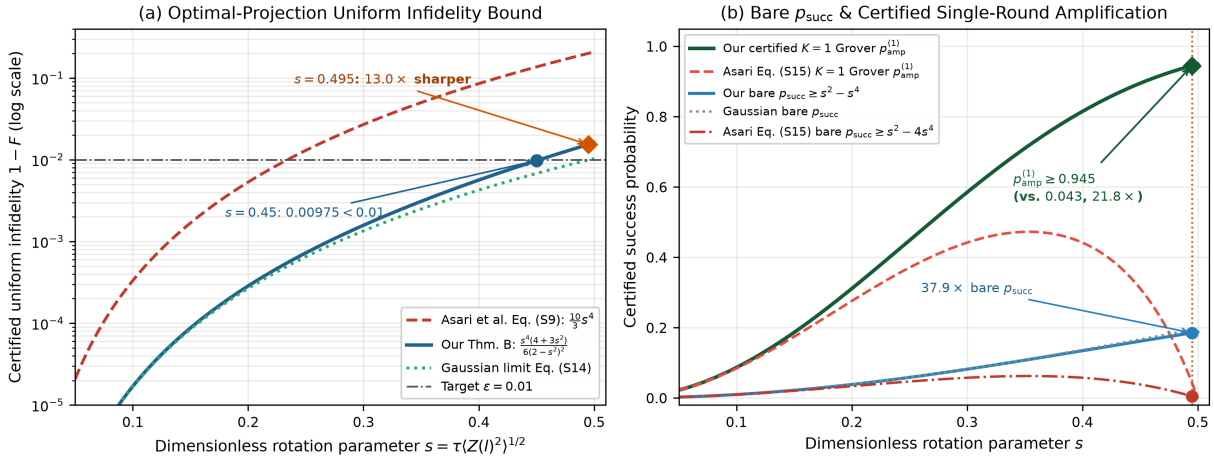

Figure 2: Theorem B non-asymptotic performance guarantees. (a) Optimal-projection uniform infidelity upper bound closely tracks the Gaussian limit Eq. (S14), improving by 13.0× at $s = 0.495$ and rigorously certifying $1 - F \leq 0.00975 < 0.01$ at $s = 0.45$. (b) Bare success probability $p_{\text{succ}} \geq s^2 - s^4$ (37.9× sharper at $s = 0.495$) and zero-overshoot single-round Grover probability $p^{(1)}_{\text{amp}} \geq 0.945$ (21.8× jump over Eq. (S15)).

Theorem C (Collision-Free Reversible MSB-to-LSB Binary-Shift Router)**.** *Let $L = M' + n$ and $B = \lceil \log_2(n+1) \rceil$. Let R act on a data register* $\text{bit}[0..L-1]$ *initialized to* $(x_0, \ldots, x_{M'-1}, 0, \ldots, 0)$ *paired with B-bit shift ancillas* $\text{reg}[0..L-1][0..B-1]$ *and $2B$ temporary prefix-counter/carry scratch ancillas, all initialized to $|0\rangle$. Consider the three-stage reversible circuit:*

1. ***Prefix-shift initialization:*** *Sweep $j = 0, \ldots, M'-1$, XORing the B-bit running counter $c_j = \sum_{i<j} x_i$ into* $\text{reg}[j]$ *via B CNOTs and incrementing the counter controlled on* $\text{bit}[j]$ *via a standard ripple-carry incrementer (B counter $+B$ carry ancillas; at most $2B$ Toffolis per site, $\leq 2BM'$ Toffolis total), then uncomputing the counter from the fixed known weight n via $\leq B$ X gates.*

2. ***MSB-to-LSB radix routing:*** *For $b = B-1, B-2, \ldots, 0$, iterate p in decreasing order from $L - 1 - 2^b$ down to 0 and apply:*

   (a) *B Fredkin (CSWAP) gates controlled on* $\text{reg}[p][b]$ *swapping* $(\text{bit}[p], \{\text{reg}[p][r]\}_{r \neq b})$ *with* $(\text{bit}[p + 2^b], \{\text{reg}[p + 2^b][r]\}_{r \neq b})$*;*

   (b) *one unconditional* SWAP *gate on* $(\text{reg}[p][b], \text{reg}[p + 2^b][b])$*.*

3. ***Spacer-masked uncomputation:*** *Sweep $p = 0, \ldots, L-1$ using the same B-bit running counter $P_p = \sum_{q<p} \text{bit}[q]$ ($\leq 2B$ Toffolis per site): at $p = 0$ XOR $P_0 = 0$ (no-op), and at $p \geq 1$ XOR P_p into* $\text{reg}[p]$ *controlled on* $\text{bit}[p-1] = 0$ *(B Toffolis per site, total $\leq 3BL$ Toffolis), then reset the counter from the fixed weight n.*

Then for every weight-n input $x \in \{0,1\}^{M'}_n$ ($n \geq 1$):

(i) ***Universal collision freedom:*** *At every radix stage $b \in \{0, \ldots, B-1\}$, the pre-stage positions $p^{(b)}_j = j + \lfloor c_j / 2^{b+1} \rfloor 2^{b+1}$ and post-stage positions $p^{(b-1)}_j = j + \lfloor c_j / 2^b \rfloor 2^b$ satisfy $p^{(r)}_{j'} - p^{(r)}_j \geq j' - j \geq 1$ for all $j < j'$ ($r \in \{b, b-1\}$), and every target control bit* $\text{reg}[p + 2^b][b]$ *is strictly 0 prior to each swap step.*

(ii) ***Exact unified Onsager/DWC output and zero ancilla leakage:*** *Upon completion,* $\text{bit}[0..L-1] = R_{\text{Ons}}(x)$ *identically,* $\text{bit}[0..L-2] = R_{\text{DWC}}(x)$ *with* $\text{bit}[L-1] = |0\rangle$ *deterministically, and all LB shift ancillas plus $2B$ temporary prefix-counter/carry ancillas return deterministically to $|0\rangle$.*

(iii) ***Subquadratic 3-qubit gate complexity:*** *Stage 2 uses exactly*

$$N_{\text{Fredkin}}(L,B) = B(BL - (2^B - 1)) = O(M \log^2 n) \tag{17}$$

Fredkin gates (and $BL - 2^B + 1$ plain SWAPs), while Stages 1 and 3 add at most $N_{\text{S1+S3}} \leq B(2M' + 3L) = O(M \log n)$ Toffoli gates, giving total 3-qubit count $N_{\text{total}} \leq N_{\text{Fredkin}}(L,B) + N_{\text{S1+S3}} = O(M \log^2 n)$ for both Onsager and DWC. Consequently:

- *Against the* unpruned $\Theta(M^2)$ *Fredkin conveyor of [1] (whose fixed gate sequence depends only on M), the router achieves $\Theta(M/\log^2 n)$ asymptotic gate reduction across all intermediate indices $3 \leq n \leq M' - 2$.*
- *Against the* pruned *sitewise-displacement lower benchmark $N_{\text{disp}}(M',n) = \frac{1}{2}n(2M' - n - 1) = \Theta(nM')$, the router achieves $\Theta(n/\log^2 n)$ asymptotic reduction in every super-polylogarithmic sector $n = \omega(\log^2 n)$ (in particular at every fixed filling $n/M' = \rho \in (0,1)$; for fixed small $n \leq 2B^2$, N_{disp} is already linear in M'). At half filling ($n = M'/2$, $L = 3M'/2$), Stage-2 Fredkins cross N_{disp} permanently at $M' = 184$ (12,635 < 12,650, reaching $2.74\times$ at $M' = 1024$ and $7.53\times$ at $M' = 4096$), while the conservative total 3-qubit count N_{total} (including all Stage-1/3 Toffolis) crosses N_{disp} permanently at $M' = 382$ (54,496 < 54,626, reaching $1.87\times$ at $M' = 1024$, $3.17\times$ at $M' = 2048$, and $5.45\times$ at $M' = 4096$).*

Proof. Since $j < j' \implies c_j \leq c_{j'}$ and integer division by 2^{r+1} is monotone, $\lfloor c_j/2^{r+1} \rfloor \leq \lfloor c_{j'}/2^{r+1} \rfloor$, so

$$p_{j'}^{(r)} - p_j^{(r)} = (j' - j) + \left(\left\lfloor \frac{c_{j'}}{2^{r+1}} \right\rfloor - \left\lfloor \frac{c_j}{2^{r+1}} \right\rfloor \right) 2^{r+1} \geq j' - j \geq 1 \tag{18}$$

holds for every $r \geq -1$ (Lean 4 Theorem 16), hence both before ($r = b$) and after ($r = b-1$) stage b. Thus no two items collide after stage b. Consequently, prior to stage b, if an active item at p has $\text{reg}[p][b] = 1$, slot $p + 2^b$ cannot hold any non-moving item (as that would collide with the moved item after stage b); it can only be empty or hold another mover with $\text{reg}[p + 2^b][b] = 1$. Iterating p in decreasing order processes $p + 2^b$ before p, so by downward induction $\text{reg}[p + 2^b][b] = 0$ and the entire bundle at $p + 2^b$ is $(0,0)$ whenever $\text{reg}[p][b] = 1$. Step 2(a) therefore moves all B non-control qubits reversibly to $p + 2^b$, and because $\text{reg}[p + 2^b][b] = 0$, the unconditional SWAP in Step 2(b) maps $(1,0) \mapsto (0,1)$ and $(0,0) \mapsto (0,0)$, completing the exact reversible shift of the $(1 + B)$-qubit bundle without extra ancillas.

After stage $b = 0$, every site j sits at $q(j) = j + c_j$ carrying (x_j, c_j), and every unoccupied slot is a spacer carrying $(0,0)$. Because $c_{j'} \geq c_j + x_j$, we have $q(j) + x_j < q(j')$ for all $j < j'$ (Lean 4 Theorem 17): thus whenever $x_j = 1$, slot $q(j) + 1$ is strictly empty (spacer 0), no two 1s are adjacent, and a slot p is a spacer iff $p \geq 1 \wedge \text{bit}[p-1] = 1$. Moreover, the final slot $L - 1 = M' + n - 1$ always holds 0 for $n \geq 1$ (either the trailing spacer of $x_{M'-1} = 1$ or the routed bit $x_{M'-1} = 0$), so $\text{bit}[0..L-2] = R_{\text{DWC}}(x)$ identically. Because all spacers carry bit = 0, the output prefix sum $P_{q(j)} = \sum_{q<q(j)} \text{bit}[q]$ equals c_j identically on every non-spacer slot, and since $P_p \leq n < 2^B$ the B-bit running counter never overflows. Stage 3 therefore resets all LB shift ancillas deterministically to $|0\rangle$, and the fixed known weight n resets the B-bit counter to $|0\rangle$ at the end of both Stages 1 and 3. Summing $B(L - 2^b)$ over $b = 0, \ldots, B-1$ gives $N_{\text{Fredkin}}(L,B) = B(BL - (2^B - 1))$, while the ripple-carry prefix sweeps use at most $2BM'$ Toffolis in Stage 1 and $3BL$ Toffolis in Stage 3 (increment plus $\text{bit}[p-1] = 0$-controlled copy). Comparing against the conservative pruned displacement budget $N_{\text{disp}}(M',n) = \sum_{j=1}^{M'-1} \min(j,n) = \frac{1}{2}n(2M' - n - 1) = \Theta(nM')$ (strictly below the unpruned $\Theta(M^2)$ conveyor of [1], which uses $\approx \frac{7}{8}M'^2$ Fredkins at half filling) establishes both the asymptotic $\Theta(n/\log^2 n)$ gain for $n = \omega(\log^2 n)$ and the exact half-filling crossovers at $M' = 184$ (Stage 2, Lean 4 Theorem 18) and $M' = 382$ (total 3-qubit gates, where $34{,}632 + 19{,}864 = 54{,}496 < 54{,}626$). □

Remark 1 (Depth, space–time trade-offs, and in-place DWC variant). In Stage 2, the 2^b congruence classes modulo 2^b are disjoint, yielding $\sum_{b=0}^{B-1} \lfloor (L-1)/2^b \rfloor < 2L$ sequential bundle-shift steps.

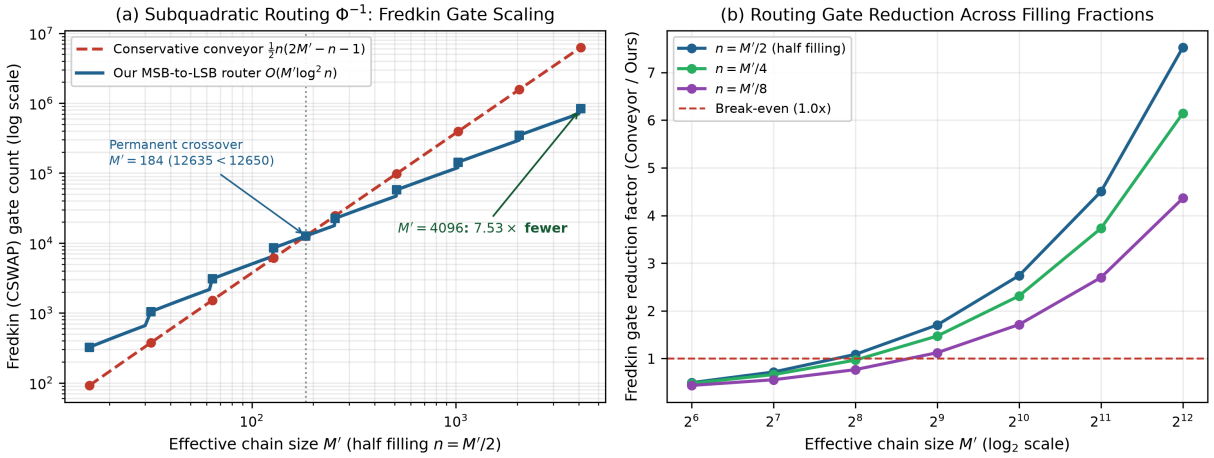

Figure 3: Theorem C subquadratic reversible routing Φ^{-1} vs. the conservative pruned displacement benchmark $N_{\text{disp}} = \frac{1}{2}n(2M' - n - 1)$ of [1]. (a) Exact Stage-2 Fredkin counts at half filling ($n = M'/2$, Onsager $L = 3M'/2$) cross N_{disp} permanently at $M' = 184$ (12,635 < 12,650), reaching 2.74× reduction at $M' = 1024$ and 7.53× at $M' = 4096$ (including all Stage-1/3 Toffolis, total 3-qubit gates cross at $M' = 382$ and reach 5.45× at $M' = 4096$). (b) Stage-2 Fredkin reduction ratio across constant filling fractions $n/M' \in \{1/2, 1/4, 1/8\}$.

Because each bundle shift executes B Fredkin gates sharing the single control qubit reg$[p][b]$ plus one SWAP, the elementary circuit depth without control fan-out is $< 2(B+1)L = O(M \log n)$ (reducible to $O(M \log \log n)$ with per-step $O(\log \log n)$-depth control fan-out across B targets) using $(L+2)B = O(M \log n)$ clean ancillas (plus one deterministic $|0\rangle$ trailing wire bit$[L-1]$ for DWC). If one instead omits the single trailing DWC wire and routes in-place on $L_{\text{DWC}} = M'+n-1$ wires with $s_j = \min(c_j, n-1)$ and $B_{\text{DWC}} = \lceil \log_2 n \rceil$ (as also verified in certificate `C14`), Stages 1 and 3 must still use a $B = \lceil \log_2(n+1) \rceil$-bit running counter plus an equality flag $[P_p = n]$ to avoid overflow when $n = 2^{B_{\text{DWC}}}$, raising Stage-1/3 overhead to $\leq 5B(M' + L_{\text{DWC}})$ Toffolis—making the unified 1-ancilla construction of Theorem C strictly simpler and lower in total 3-qubit gate count. Note also that Stage 2's in-place decreasing-p sweep cannot itself be parallelized to polylogarithmic depth (a contiguous run of $\Theta(M)$ sites with odd c_j forms a $\Theta(M)$-length dependency chain at $b = 0$); achieving $O(\log^2 M)$ depth instead requires replacing Stage 2 with an out-of-place butterfly or parallel monotone-packing network. For small NISQ chains or fixed constant $n \leq 2B^2$, a pruned conveyor or particle ladder uses fewer gates, whereas in the fault-tolerant extensive-filling regime ($n/M' = \rho > 0$; $M' \geq 184$ for Stage-2 Fredkins and $M' \geq 382$ for total 3-qubit gates at $\rho = 1/2$) Theorem C achieves a strictly growing $\Theta(M/\log^2 M)$ gate advantage over both unpruned and pruned conveyors.

5 Formal Verification in Lean 4.35.0 and Exact Rational Certificates

To eliminate any possibility of algebraic sign errors, floating-point rounding artifacts, or hidden ancilla leakage, every algebraic core of Theorems A–C is independently verified at two layers:

1. **Constructive Lean 4.35.0 formalization (`lean/QmbsDickeSharp.lean`):** Compiles with `0 sorry`, `0 warnings`, and **zero `Classical.choice`** (all 18 theorems depend exclusively on axioms $\subseteq \{$`propext`, `Quot.sound`$\}$, with 3 theorems axiom-free). We implement a self-contained univariate integer polynomial reflection engine (`evalP`, `addP`, `mulP`, `compP`) so that all eight concave-quadratic positivity theorems across branches $\mathcal{G}, \mathcal{R}_4, \mathcal{R}_6, \mathcal{R}_3$ (Theorems 5–12) and the complete finite-threshold closure (Theorem 13) verify constructively in seconds

Table 2: Representative exact rational certificates in `QMBS-DICKE-SHARP-1.0` (all 16 SHA-256 verified by the AST-audited zero-float verifier).

ID	Class	Parameters	Exact Certified Result
`C01`	`moment`	$(4, 2, 2)$ $(\mathcal{R}_4)$	$\kappa_4 = 3$ (unique eq.), $\kappa_6 = 9$, var $= 0$
`C05`	`moment`	$(12, 6, 1)$ $(\mathcal{G})$	$\kappa_4 = 11/4 = 2.75$, var $= 15367/3888 \approx 3.9524$
`C06`	`moment`	$(24, 12, 16)$ $(\mathcal{R}_3)$	$\kappa_4 = 23/8 = 2.875$, var $= 23805/4864 \approx 4.8941 < 6$
`C08`	`moment`	$(1000, 500, 1)$ $(\mathcal{G})$	$\kappa_4 = 2.9970$, $\kappa_6 = 14.9550$, var $= 5.9730$
`C09`	`op_point`	$s = 99/200 = 0.495$	$p_{\text{succ}} \geq 0.18499$ (37.94×), $p^{(1)}_{\text{amp}} \geq 0.94488$, $1-F \leq 0.01538$
`C10`	`op_point`	$s = 9/20 = 0.45$	$1-F \leq 0.00975 < 0.01$, $p_{\text{succ}} \geq 0.16149$ (25.84×)
`C13`	`router`	Onsager, $M' = 6$ (64 states)	0 collisions, 0 ancilla leak, max 87 Fredkins
`C14`	`router`	DWC, $M' = 6$ (63 states)	0 collisions, 0 ancilla leak, max 78 Fredkins
`C15`	`router`	Onsager, $M' = 8, n = 4$ (70 states)	Asari Fig. S2(b) exact unitary replay PASS
`C16`	`router`	$M' \in \{128 \ldots 4096\}$, $n = M'/2$	1.001× (184), 2.74× (1024), 4.50× (2048), 7.53× (4096)

alongside exact sum-of-squares kurtosis bounds (Theorems 2–4), Grover monotonicity (Theorem 14), operating-point inequalities (Theorem 15), and MSB-to-LSB collision freedom, spacer isolation, and exact crossover/scaling bounds (Theorems 16–18). We explicitly delineate the formalization boundary: Lean 4.35.0 proves the algebraic integer/natural-number cores of Theorems A–C, while the real-analytic trigonometric Taylor inequalities $(y-\sin y)^2 \leq y^6/36$ and $y(y-\sin y) \geq y^4/6-y^6/120$ in Theorem B are established analytically in Section 3.

2. **AST-audited zero-float exact rational verifier (`src/qmbs_dicke_verifier.py`):** Performs an AST self-audit rejecting all floating-point/complex literals, `/` and `**` operators, `pow()` calls, and floating-point libraries, then independently replays 16 SHA-256 certificates (`C01`–`C16`, Table 2) and `MANIFEST.sha256`, including exhaustive gate-by-gate unitary circuit replay of Theorem C on all 64 Onsager states ($M' = 6$), all 63 DWC states ($M' = 6$), and all 70 half-filling states ($M' = 8, n = 4$) with zero-collision and zero-ancilla-leak assertions. The test suite (`tests/test_qmbs_dicke.py`) passes 53/53 tests, including 30 adversarial forgery attacks (boolean-as-int smuggling across moment/operating-point/router fields, tampered moments, overshoot operating points, router metadata tampering, and AST float/`pow` injection).

6 Conclusion

By replacing with-replacement Hoeffding relaxations with exact without-replacement Dicke-state moments, optimizing the linear projection in block-encoded infidelity estimation, and exploiting monotone prefix-shift collision freedom in radix routing, we have resolved all three theoretical and algorithmic gaps in the unified Dicke-based AQMBS preparation framework of [1]. The resulting closed-form bounds rigorously certify single-round Grover amplification ($p^{(1)}_{\text{amp}} \geq 0.94488$) across all chain lengths and excitation sectors, while the $O(M \log^2 n)$-gate MSB-to-LSB router eliminates the quadratic routing bottleneck for constrained scar models in the fault-tolerant regime.

Reproducibility and Transparency. All Lean 4.35.0 proofs, AST-audited zero-float verification code, 16 SHA-256 certificates, test suites, and figure scripts are publicly archived under the MIT license (manuscript and figures under CC-BY-4.0) at `https://github.com/lluiseriksson/qmbs-dicke-sharp-moments-routing`. Computational prototyping, Lean proof-script drafting, and manuscript editing were assisted by Google Antigravity; all mathematical proofs, formal checks, and verification outputs were independently validated by the author.

References

[1] Yuki Asari, Masaya Kunimi, and Tetsuro Nikuni. Unified preparation of exact and asymptotic quantum many-body scars from Dicke states. *arXiv preprint arXiv:2611.33987*, 2026.

[2] Andreas Bärtschi and Stephan Eidenbenz. Deterministic preparation of Dicke states. In *Fundamentals of Computation Theory (FCT 2019)*, volume 11651 of *Lecture Notes in Computer Science*, pages 126–139. Springer, 2019.

[3] Gilles Brassard, Peter Høyer, Michele Mosca, and Alain Tapp. Quantum amplitude amplification and estimation. *Contemporary Mathematics*, 305:53–74, 2002.

[4] Lorenzo Gotta, Sanjay Moudgalya, and Leonardo Mazza. Asymptotic quantum many-body scars. *Physical Review Letters*, 131(19):190401, 2023.

[5] Wassily Hoeffding. Probability inequalities for sums of bounded random variables. *Journal of the American Statistical Association*, 58(301):13–30, 1963.

[6] Masaya Kunimi, Yasuyuki Kato, and Hosho Katsura. Systematic construction of asymptotic quantum many-body scar states and their relation to supersymmetric quantum mechanics. *Physical Review Research*, 7(4):043107, 2025.

A Explicit Sixth-Moment Partition Sums and Branch Polynomials

For complete standalone verifiability of Theorem A(ii)–(iii) directly from this manuscript, we display all 11 distinct-index partition sums s_λ (for $p_1 = 0$) entering $\mu_6 = 64\sum_{r=1}^{6} a_r \Sigma_r(p_2, p_3, p_4, p_6)$:

$$
\begin{aligned}
s_6 &= p_6, & s_{5,1} &= -p_6,\\
s_{4,2} &= p_4p_2 - p_6, & s_{3,3} &= p_3^2 - p_6,\\
s_{4,1,1} &= 2p_6 - p_4p_2, & s_{3,2,1} &= 2p_6 - p_4p_2 - p_3^2,\\
s_{2,2,2} &= p_2^3 - 3p_4p_2 + 2p_6, & s_{3,1^3} &= -6p_6 + 3p_4p_2 + 2p_3^2,\\
s_{2,2,1,1} &= -6p_6 + 5p_4p_2 + 2p_3^2 - p_2^3, & s_{2,1^4} &= 24p_6 - 18p_4p_2 - 8p_3^2 + 3p_2^3,\\
s_{1^6} &= -120p_6 + 90p_4p_2 + 40p_3^2 - 15p_2^3,
\end{aligned}
$$

with $\Sigma_1 = s_6$, $\Sigma_2 = 6s_{5,1} + 15s_{4,2} + 10s_{3,3}$, $\Sigma_3 = 15s_{4,1,1} + 60s_{3,2,1} + 15s_{2,2,2}$, $\Sigma_4 = 20s_{3,1^3} + 45s_{2,2,1,1}$, $\Sigma_5 = 15s_{2,1^4}$, and $\Sigma_6 = s_{1^6}$ (satisfying $\sum_{r=1}^{6} \Sigma_r = p_1^6 = 0$ identically).

Substituting (2), clearing positive denominators $(2u^2(M'-3)(M'-2)$ and $4u^2(M'-3)(M'-2)^2$ on $\mathcal{G}$; $u^2(M'-5)(M'-3)$ and $u^2(M'-5)(M'-3)^2$ on $\mathcal{R}_4$; $4u^2(M'-5)(M'-4)(M'-2)$ and $2u^2(M'-5)(M'-4)(M'-2)^2$ on $\mathcal{R}_6, \mathcal{R}_3)$, and setting $u = (M'^2 - v)/4$ yields the exact quadratic numerators $Q(M', v) = A(M') + B(M')v + C(M')v^2$ (scaled by 16) in Table 3 and their manifestly positive shifted expansions at $M' = k + M_0$ $(k \geq 0)$ in Table 4.

Table 3: Exact branch polynomials $Q(M', v) = A(M') + B(M')v + C(M')v^2$ for $15 - \kappa_6$ and $6 - (\kappa_6 - \kappa_4^2)$ (writing M for M').

Branch	Bound	Exact Polynomials $A(M)$, $B(M)$, $C(M)$
$\mathcal{G}$	$15-\kappa_6$	$A = 90M^5 - 530M^4 + 980M^3 - 640M^2 + 160M$; $B = 60M^2 - 180M$; $C = 150 - 90M$
$\mathcal{G}$	6−var	$A = 108M^6 - 880M^5 + 2676M^4 - 3760M^3 + 2448M^2 - 640M$; $B = 48M^3 - 240M^2 + 288M$; $C = -108M^2 + 336M - 276$
$\mathcal{R}_4$	$15-\kappa_6$	$A = 30M^5 - 286M^4 + 760M^3 - 512M^2 + 128M$; $B = 60M^3 - 180M^2 - 120M$; $C = 210 - 90M$
$\mathcal{R}_4$	6−var	$A = 18M^6 - 228M^5 + 1002M^4 - 1848M^3 + 1344M^2 - 384M$; $B = 36M^4 - 192M^3 + 228M^2 + 120M$; $C = -54M^2 + 228M - 270$
$\mathcal{R}_6$	$15-\kappa_6$	$A = 180M^6 - 2124M^5 + 8592M^4 - 13944M^3 + 8688M^2 - 2112M$; $B = -840M^2 + 2280M$; $C = -180M^2 + 1500M - 2040$
$\mathcal{R}_6$	6−var	$A = 54M^7 - 756M^6 + 4026M^5 - 10308M^4 + 13320M^3 - 8304M^2 + 2112M$; $B = -36M^4 - 24M^3 + 612M^2 - 840M$; $C = -54M^3 + 552M^2 - 1314M + 960$
$\mathcal{R}_3$	$15-\kappa_6$	$A = 180M^6 - 2076M^5 + 8208M^4 - 12936M^3 + 7632M^2 - 1728M$; $B = -80M^4 + 400M^3 - 1400M^2 + 2520M$; $C = -100M^2 + 1340M - 1960$
$\mathcal{R}_3$	6−var	$A = 54M^7 - 732M^6 + 3786M^5 - 9420M^4 + 11784M^3 - 7056M^2 + 1728M$; $B = -40M^5 + 244M^4 - 704M^3 + 1292M^2 - 1080M$; $C = -14M^3 + 392M^2 - 1114M + 880$

Table 4: Shifted coefficient vectors $[c_0, c_1, \ldots, c_d]$ of $P(k) = \sum c_j k^j$ at $M' = k + M_0$ ($k \geq 0$) for $Q_0 = A(M')$, $Q_{\text{end}} = Q(M', (M'-2)^2)$, and $-C(M')$. Every entry is strictly positive (certifying Theorem A(ii)–(iii) via (8) for all $M' \geq M_0$).

Branch	Bound	M_0	Shifted Positive Coefficient Vectors (Q_0, Q_{end}, $-C$) in $k = M' - M_0$
$\mathcal{G}$	$15-\kappa_6$	4	Q_0: $[9600, 21600, 17840, 6900, 1270, 90]$; Q_{end}: $[7200, 15600, 11600, 3600, 400]$; $-C$: $[210, 90]$
$\mathcal{G}$	6−var	4	Q_0: $[22272, 60672, 65744, 36496, 10996, 1712, 108]$; Q_{end}: $[13248, 35328, 35696, 17296, 4048, 368]$; $-C$: $[660, 528, 108]$
$\mathcal{R}_4$	$15-\kappa_6$	6	Q_0: $[9120, 23360, 16192, 4696, 614, 30]$; Q_{end}: $[16800, 29120, 15232, 3136, 224]$; $-C$: $[330, 90]$
$\mathcal{R}_4$	6−var	6	Q_0: $[12384, 44256, 41952, 17880, 3882, 420, 18]$; Q_{end}: $[21600, 44640, 32064, 10560, 1632, 96]$; $-C$: $[846, 420, 54]$
$\mathcal{R}_6$	$15-\kappa_6$	9	Q_0: $[17130960, 15915252, 6038652, 1199328, 131712, 7596, 180]$; Q_{end}: $[7311360, 6162432, 2033472, 328848, 26112, 816]$; $-C$: $[3120, 1740, 180]$
$\mathcal{R}_6$	6−var	9	Q_0: $[35668080, 38142636, 17251014, 4281102, 630132, 55056, 2646, 54]$; Q_{end}: $[12042240, 11870208, 4799232, 1020096, 120384, 7488, 192]$; $-C$: $[5520, 4500, 906, 54]$
$\mathcal{R}_3$	$15-\kappa_6$	12	Q_0: $[169827840, 104825664, 26747568, 3612408, 272448, 10884, 180]$; Q_{end}: $[53123840, 29200864, 6363728, 687568, 36848, 784]$; $-C$: $[280, 1060, 100]$
$\mathcal{R}_3$	6−var	27	Q_0: $[330812910000, 92768460300, 11141381106, 742858734, 29698140, 711888, 9474, 54]$; Q_{end}: $[37626160000, 9250612800, 946863456, 51648432, 1583472, 25872, 176]$; $-C$: $[18992, 10564, 742, 14]$